Electronic Supplementary Information

Spray Processing of TiO_2 Nanoparticle/Ionomer Coatings on Carbon Nanotube Scaffolds for Solid-State Supercapacitors

Chun Huang*, Neil P. Young and Patrick S. Grant

Department of Materials, University of Oxford, Parks Road, Oxford, OX1 3PH, UK

Additional image of the solid-state supercapacitor:

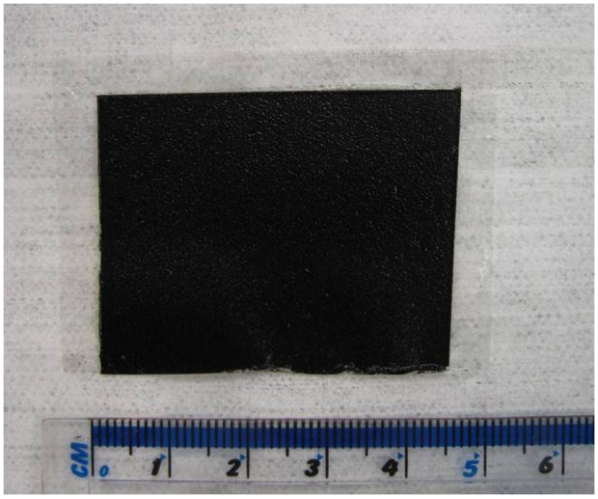

Figure S1: An image of the as-sprayed 4.5 cm x 4 cm solid-state supercapacitor with MWNT/TiO_2/ionomer electrodes.

Additional data on chemistry properties:

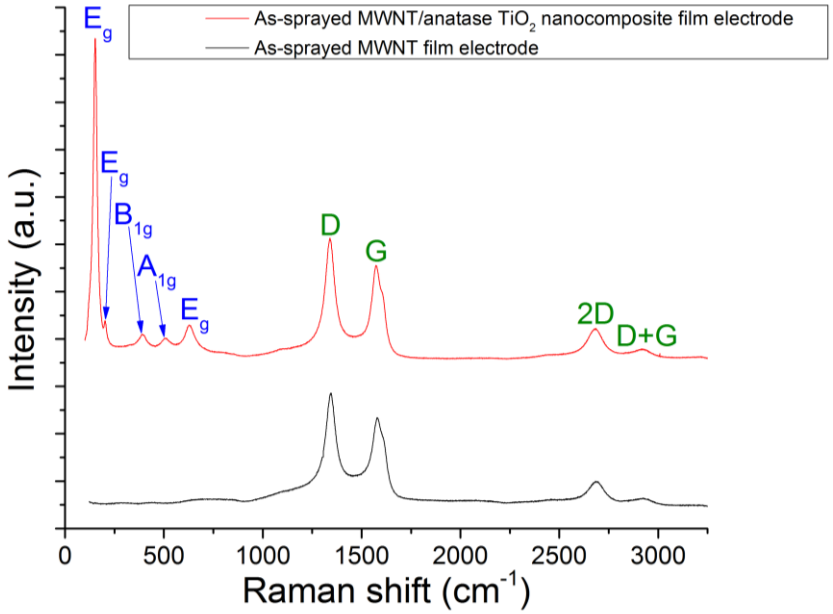

Figure S2: Raman spectra for an as-sprayed MWNT film electrode and an as-sprayed MWNT/anatase TiO_2 nanocomposite film electrode.

Fig. S2 shows the Raman spectra for both as-sprayed MWNT-only and MWNT/anatase TiO_2 electrodes. Both spectra showed a G band at 1582 cm^{-1} corresponding to the -C-C- bond in the wrapped graphene plane, and a D band at 1330 cm^{-1} corresponding to the C-related defects within the as-received MWNTs. The 2D and G+D bands were typical for MWNTs [1]. The peaks in the 100-700 cm^{-1} region confirmed the presence of anatase TiO_2 with a dominating E_g mode at 147 cm^{-1} [2], indicating that as expected the as-sprayed nanocomposite electrode preserved the structures of both MWNTs and anatase TiO_2.

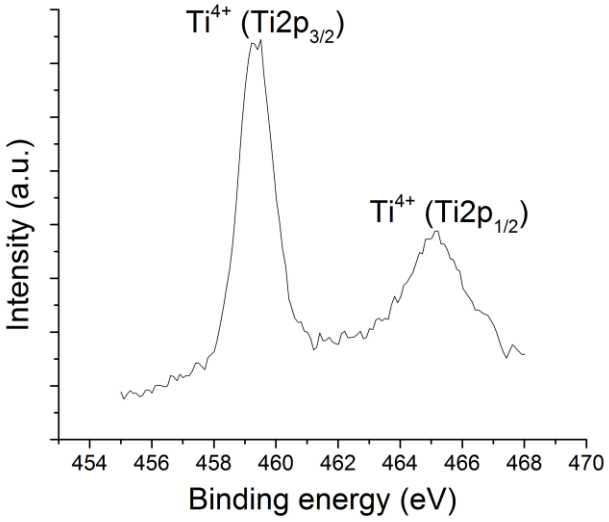

Figure S3: XPS spectrum of detailed Ti_{2p} scan for the as-received TiO_2 powder.

Fig. S3 shows two peaks at 465 and 459.3 eV corresponded to the characteristic Ti $2p_{1/2}$ and Ti $2p_{3/2}$ peaks of Ti^{4+} [3] seen in all of the as-sprayed electrodes.

Additional data on electrochemical properties:

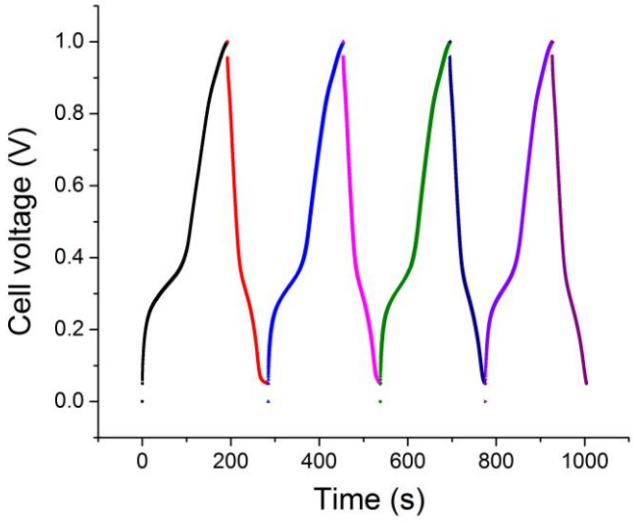

Figure S4: Galvanostatic charge/discharge curves of a solid-state supercapacitor with MWNT/TiO_2/ionomer electrodes at 1 A g^{-1}.

Fig. S4 shows the galvanostatic charge and discharge cycles of a solid-state supercapacitor with MWNT/TiO_2/ionomer electrodes at 1 A g^{-1}, with an estimated capacitance of 460 F g^{-1} (81 mF cm^{-2}).

Additional data on dehydration-rehydration behaviour:

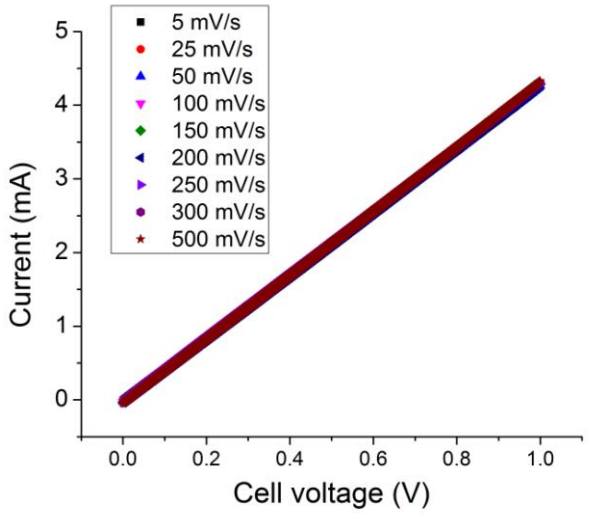

Figure S5: CV curves of the supercapacitor after dehydrating in vacuum at 105 °C for 16 hrs.

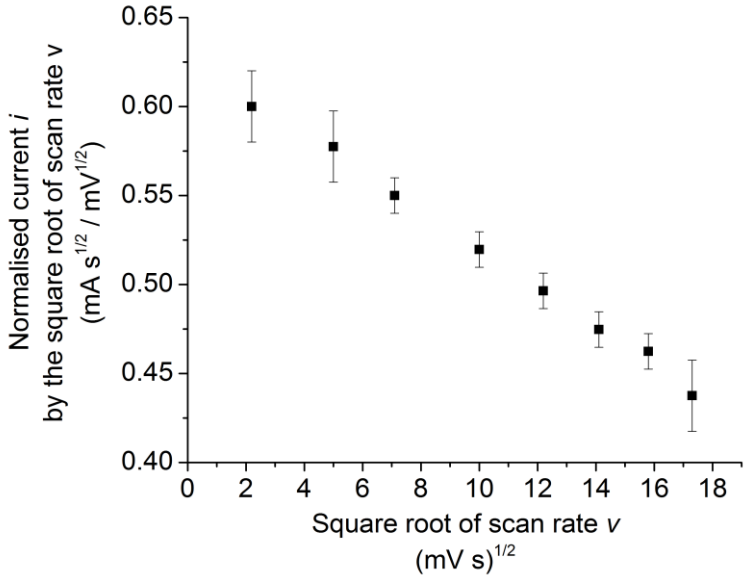

Figure S6: A plot of CV normalised peak current against the square root of scan rate for the rehydrated solid-state supercapacitor with MWNT/TiO_2/ionomer electrodes over steam for 2 hrs.

The pseudo-capacitive contribution of an electrode material can be shown by the peak current response in a CV curve in Fig. 5(e) normalised by the square root of scan rate, as shown in Fig. S6. The current response can be expressed as [4]:

$$i/v^{1/2} = k_1 v^{1/2} + k_2 \qquad (1)$$

where $v^{1/2}$ is the square root of scan rate, $i/v^{1/2}$ is the normalised peak current by the square root of scan rate, k_1 is a constant corresponding to the EDLC contribution, and k_2 is a constant corresponding to the pseudo-capacitive contribution.

The data in Fig. S6 fitted closely to a linear relationship showing that the normalised peak current was proportional to the square root of scan rate, indicating that the reaction was diffusion controlled and pseudo-capacitive [4]. The current response at the fastest scan rate of 500 mV s^{-1} was not used as the scan time was too fast for redox reactions to complete. The linear relationship and a slope of k_1 = 0.01 and an intercept k_2 = 0.625 mA $s^{1/2}$ $mV^{(-1/2)}$ indicated hydroxyl groups were re-introduced to the dehydrated solid-state supercapacitor after rehydration, restoring their pseudo-capacitive contribution.

Experimental:

Fabrication of solid-state supercapacitors by a single-step spray approach

Membranes (Nafion, 70 μm thickness, Du Pont) were pre-treated by immersing in 1 M H_2SO_4 at 60 °C for 30 min. Nafion is a functionalised polymer bearing negatively charged perfluorosulfonate (-SO_2F-) groups in the main structure, promoting proton hopping through -$SO_3^-H^+$- groups [5]. An aqueous suspension of 2 mg ml^{-1} MWNTs (Bayer MaterialScience), 1 mg ml^{-1} ~30 nm TiO_2 nanoparticles (Sigma-Aldrich), 0.1 wt% sodium dodecylbenzenesulfonate (SDBS, Sigma-Aldrich) and 50 wt% Nafion ionomer (Sigma-

Aldrich) in 0.5 M H_2SO_4 was prepared by sonication at 600 W and 20 kHz for 15 min. The stable suspension was pumped at 3 ml ml^{-1} into a spray head, and atomised using compressed air at 310 kPa to be deposited onto one side of the membrane which was maintained at 100 °C on a heating plate/vacuum chuck. The membrane with one side covered with the sprayed electrode was then flipped and sprayed on the other side using the identical procedure. The thickness of each electrode was controlled by the spray time to be ~10 μm. Cu foil current collectors of 10 μm thickness were added onto the two sides of the supercapacitor by gentle manual pressing. Graphite coated Cu and indium tin oxide (ITO) coated glass current collectors were also tested in order to assess any significant underlying Cu reaction in the potential range of interest and was demonstrated to be negligible [6].

Characterisation

The weight of electrodes was measured by a microbalance (Sartorius) with 0.01 mg accuracy and electrode thickness using a Dektak 6M profilometer (Veeco Instruments Inc). Specific surface area (SSA) was measured for a mixed powder of MWNTs and TiO_2 nanoparticles using the Brunauer-Emmett-Teller (BET) method with a Micrometrics Gemini VI. The sample was prepared by degassing at 150 °C under N_2 atmosphere overnight to remove physically adsorbed molecular species before the measurements were taken. The conductivity of the electrodes was measured by using a standard four-point probe configuration and a Keithley 220 programmable current source meter and an Agilent 34420A digit nano volt/micro ohm meter, on the electrodes deposited on Si wafers.

The surface chemistry of the as-received TiO_2 and the sprayed electrodes were analysed by XPS in an ion pumped VG Microtech CLAM 4 multi-channel detecting analyser equipped with a Mg K_{α} source. The XPS analyser operated at a constant pass energy of 100 eV for wide scans and 20 eV for detailed scans. The sprayed electrode chemistry was also

investigated using Raman spectroscopy (Horiba LabRAM ARAMIS) with a 532 nm wavelength laser.

The surface morphology of the electrodes was examined by SEM (JEOL 840F at 3 kV), and TEM (JEOL 2010 at 200 kV) and HRTEM (JEOL 3000F at 300 kV). Electrochemical testing was performed on both conventional three-electrode configuration and solid-state full cell configuration using a Reference 600/EIS300 Gamry potentiostat/galvanostat. In the three-electrode configuration, the MWNT/TiO_2/ionomer electrode was the working electrode, while a Pt wire and a Ag/AgCl electrode were used as the counter and reference electrodes, respectively.

Calculation of performance parameters of solid-state supercapacitors:

For CV investigations, specific capacitance was estimated according to [7]

$$C = \frac{1}{mv(V_a - V_c)} \int_{V_a}^{V_c} I(V)dV \qquad (2)$$

where C is the specific capacitance (F g^{-1}), m is the mass of one electrode (g), v is the scan rate (V s^{-1}), V_a-V_c represents the potential window (V), and I is either the charging or discharging current (A). The capacitances estimated from the CV charging and discharging current for this symmetrical supercapacitor were similar, since no resolvable irreversible reaction took place on either anodic or cathodic scan [8].

For galvanostatic charge/discharge investigations, the capacitance was estimated from the slope of the discharge curve according to Equation 3, where the discharge current I (A) is normally used and t is the corresponding discharge time (s) from a voltage V (V), and only the linear part of discharge curve was used to estimate capacitance [8]:

$$C = \frac{I}{m\frac{dV}{dt}} \quad (3)$$

The energy density E and maximum power density P can be expressed as [9]:

$$E = \frac{1}{2}\frac{CV^2}{m} \quad (4)$$

$$P = \frac{V^2}{4R_s m} \quad (5)$$

where R_s is the equivalent internal resistance.

References in ESI

[1] M. Zdrojek, W. Gebicki, C. Jastrzebski, T. Melin and A. Huczko, *Solid State Phenomena*, 2004, **99**, 265.

[2] G. Liu, H. G. Yang, X. Wang, L. Cheng, H. Lu, L. Wang, G. Q. M. Lu and H. M. Cheng, *J. Phys Chem C*, 2009, **113**, 21784.

[3] D. Briggs, J. T. Grant, *Surface analysis by Auger and X-ray photoelectron spectroscopy*; IM Publications, 2003.

[4] J. Wang, J. Polleux, J. Lim and B. Dunn, *J. Phys. Chem. A*, 2007, **111**, 14925

[5] M. Doyle, M. E. Lewittes, M. G. Roelofs, S. A. Perusich and R. E. Lowrey, *J. Membrane Sci.*, 2001, **184**, 257.

[6] C. Huang and P. S. Grant, *Sci. Reports*, 2013, **3 : 2393**, DOI: 10.1038/srep02393.

[7] V. Srinivasan and J. W. Weidner, *J. Power Sources*, 2002, **108**, 15.

[8] P. L. Taberna, P. Simon and J. F. Fauvarque, *J. Electrochem. Soc.*, 2003, **150**, A292.

[9] M. D. Stoller and R. S. Ruoff, *Energy Environ. Sci.*, 2010, **3**, 1294.